J Mol Model (2013) 19:2043–2048
DOI 10.1007/s00894-012-1605-y

ORIGINAL PAPER

Ab-initio study of anisotropic and chemical surface modifications of β-SiC nanowires

Alejandro Trejo · José Luis Cuevas · Fernando Salazar · Eliel Carvajal · Miguel Cruz-Irisson

Received: 6 June 2012 / Accepted: 24 September 2012 / Published online: 20 October 2012

Abstract The electronic band structure and electronic density of states of cubic SiC nanowires (SiCNWs) in the directions [001], [111], and [112] were studied by means of Density Functional Theory (DFT) based on the generalized gradient approximation and the supercell technique. The surface dangling bonds were passivated using hydrogen (H) atoms and OH radicals in order to study the effects of this passivation on the electronic states of the SiCNWs. The calculations show a clear dependence of the electronic properties of the SiCNWs on the quantum confinement, orientation, and chemical passivation of the surface. In general, surface passivation with either H or OH radicals removes the dangling bond states from the band gap, and OH saturation appears to produce a smaller band gap than H passivation. An analysis of the atom-resolved density of states showed that there is substantial charge transfer between the Si and O atoms in the OH-terminated case, which reduces the band gap compared to the H-terminated case, in which charge transfer mainly occurs between the Si and C atoms.

Keywords Nanowires · Silicon carbide · DFT · Surface passivation

Introduction

In recent years SiC nanostructures have received a great deal of attention due to their excellent chemical properties, such as their high resistance to corrosion, high Young's modulus, ability to withstand high temperatures and mechanical stresses [1], as well as their large surface areas, which make them suitable for applications in H [2] or SO_2 [3] gas sensors. SiC nanowires (SiCNWs) are special 1-D structures that are of particular interest due to their properties, which lead to potential applications of SiCNWs in spintronics [4], photocatalysis [5], capacitive humidity sensors [6], nanoelectromechanical switches [7], and nanoemitters in field emission appliances [8, 9], among others. Also, SiC is an interesting material from a chemical functionalization perspective [10] due to its binary nature, which allows multiple surface configurations with varying degrees of richness of Si or C.

SiCNWs offer interesting configurations for various chemical species to attach to its surface, but most experimental evidence suggests that their surfaces are mostly covered with SiO_2 [11–13]. Nevertheless, there are some indications that there could also be surface hydroxyl (OH) groups too [14, 15], which may arise through the apparent dissociation of water molecules at SiC surfaces [16]. There have been some theoretical studies of the electronic structure of the semiconducting and metallic properties of unpassivated and H-passivated SiCNWs [17–19], and some others that have investigated how the electronic structures of SiC nanostructures change upon interaction with O [20], but only a few studies [21, 22] have focused on variations in the electronic structure of an SiC nanocrystal with OH surface passivation.

Motivated by these experimental facts, and as a first approach to modeling the interaction of O with the SiCNW surface [23], we studied the effect of OH passivation on the electronic properties of SiCNWs using first-principles density functional theory with the generalized gradient approximation. The SiCNWs were grown in three different directions ([001], [111], and [112]), which represent the most commonly synthesized SiCNWs. A comparison was performed of the electronic band structures and densities of

A. Trejo · J. L. Cuevas · F. Salazar · E. Carvajal · M. Cruz-Irisson (✉)
Instituto Politécnico Nacional, ESIME-Culhuacan,
Av. Santa Ana 1000,
Mexico City 04430 DF, Mexico
e-mail: irisson@unam.mx

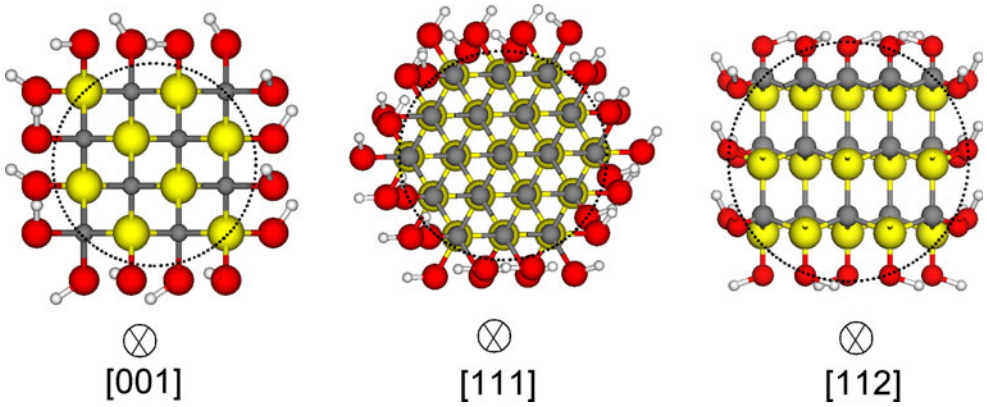

Fig. 1 Cross-section of the unrelaxed structures of the OH-passivated SiCNWs grown in the [001], [111], and [112] directions. The *yellow*, *gray*, *red*, and *white spheres* represent Si, C, O, and H atoms, respectively. The *dotted line* represents the circumference of the nanowire

states of the OH-terminated SiCNWs and the hydrogenated SiCNWs, and at the same time the diameters of the SiCNWs were varied to study quantum confinement effects in the two types of passivated SiCNWs. The results show that the band gaps are smaller for the OH-passivated SiCNWs where flat surface states near the band gap edges are observed due to localized orbitals around the OH radicals.

Model and computational details

The nanowires (NWs) were modeled using a supercell scheme [24] in which atoms outside a tube of diameter d oriented in the [001], [111], or [112] direction are removed from an otherwise perfect bulk SiC crystal, as seen in Fig. 1a–c, where the periodicity of this system in the [001], [111], and [112] directions is a, $\sqrt{3}a$, and $\sqrt{3/2}a$, respectively, where a=4.35 Å is the lattice parameter of crystalline SiC. To study the effect of confinement in these structures, three diameters were chosen for each wire direction so that the nanowires could be compared (i.e., the studied cases have similar diameters in the three directions). The diameters of the [001] NWs for which the electronic structures could be calculated were limited, so it was not possible to compare NWs with diameters >0.75 nm. All surface dangling bonds were saturated with H atoms and hydroxyl (OH) radicals to remove dangling bond states from the band gap, and to derive a first approach model of the interaction between the O in OH radicals and the NW surface. There are previous theoretical works in nanowires oriented in the [111] direction.

The electronic band structures and densities of states of all of the NWs were calculated using first-principles density functional theory based on the generalized gradient approximation with a revised version of the Perdew–Burke–Ernzerhof functional (RPBE) [25] and ultrasoft pseudopotentials [26] as implemented in the CASTEP code [27]. The cutoff energy used was 350 eV, and a highly converged set of k points was employed, with grids up to 1×1×5 in size, according to the Monkhorst–Pack scheme [28]. Finally, the nanowires were relaxed to their minimum energy configurations using the BFGS algorithm [29]; each structure was considered relaxed when all of its forces were less than 0.3 eV/Å.

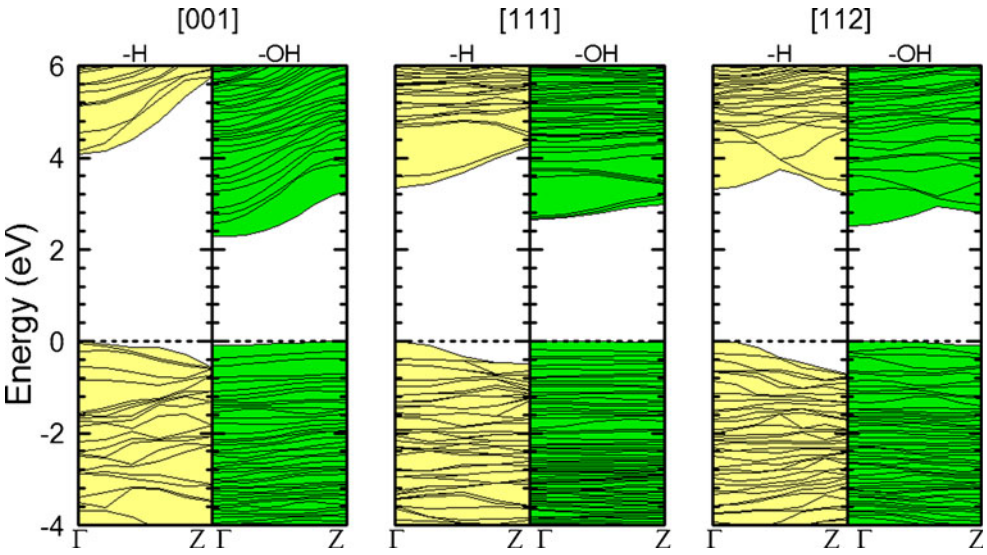

Fig. 2 Electronic band structures of H-passivated (*yellow*) and OH-passivated (*green*) SiCNWs with diameters of 0.65 nm, 0.75 nm, and 0.79 nm grown in the [001], [111], and [112] directions, respectively

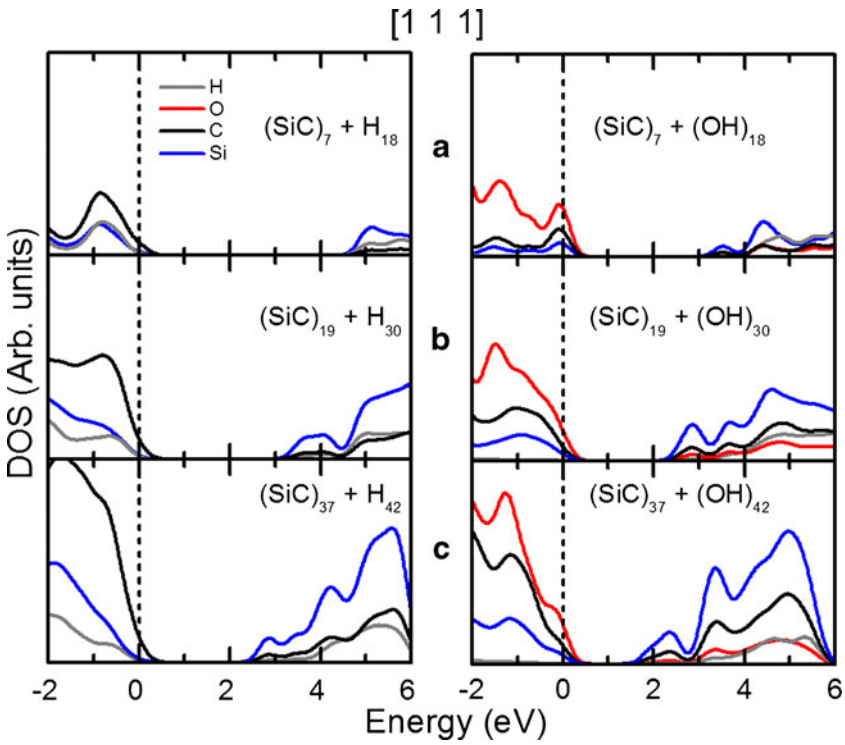

Fig. 3 Atom-resolved densities of states (DOS) for SiCNWs grown along [111]. Three NW diameters were investigated: **a** 0.65 nm, **b** 0.75 nm, and **c** 0.79 nm. The *left* (*right*) *panels* correspond to H-passivated (OH-passivated) NWs. The *blue*, *black*, *gray*, and *red lines* represent the DOS of Si, C, H, and O atoms, respectively. The number of atoms of each species per supercell is labeled in each panel

Results and discussion

In Fig. 2 we show the electronic band structures of H-terminated (yellow regions) and OH-terminated (green regions) [001]-, [111]-, and [112]-oriented SiCNWs with diameters of 0.65, 0.74, and 0.79 nm, respectively. It is apparent that all of the OH-terminated NWs have lower band gap widths than their H-passivated counterparts. This behavior has been observed previously in SiC nanocrystals [21, 22], and was attributed to the substantial charge transfer that occurs on the surfaces of the structures due to the presence of the O atoms (especially those with C–OH bonds [22]), which in turn reduces the charge transfer between Si and C, reducing the size of the band gap. Another possible explanation could be the extra *p* states introduced near the edges of the band gap by the oxygen, as described for Ge NWs [30]. It is worth noting that the OH-passivated nanowires have flat or almost flat states that arise around the maximum valence band energy, which may be due to highly localized orbitals around the oxygen atoms [23].

To analyze the electronic structures of the NWs, we calculated their atom-resolved electronic density of states (DOS). The results for the [111]-oriented NWs are shown in Fig. 3. In this figure, the panels on the left and right show the DOS for the H- and OH-terminated [111] SiCNWs, respectively. The top, middle, and bottom panels represent the DOS for NWs with diameters of 0.37 6 nm, 0.752 nm, and 1.065 nm, respectively. The number of atoms of each species per supercell is labeled in each case. It is clear that the valence-band states in the H-terminated case are dominated by contributions from the C atoms, while the principal contributor to the conduction band states is Si. A similar pattern was observed for the HOMO and LUMO orbitals of SiC quantum dots [21]. This behavior suggests that a donor–acceptor system is operating in the NWs, where Si is the

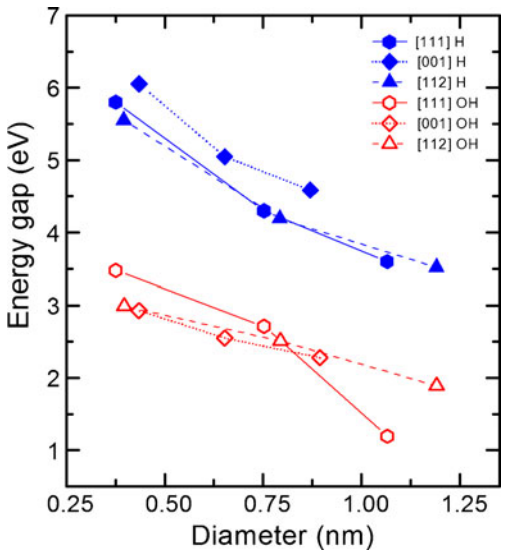

Fig. 4 Evolution of the band-gap energy as a function of the NW diameter for [001]-oriented (*solid diamonds*), [111]-oriented (*solid hexagons*), and [112]-oriented (*solid triangles*) H-passivated SiCNWs, as well as for the corresponding OH-passivated SICNWs (*open symbols*)

electron donor and C is the acceptor of the electrons that fill most of the electronic states of the C atoms in the valence band. Different behavior is observed for the OH-saturated NWs, in which the main contributors to the valence band are the O atoms and, to a lesser degree, the C atoms, even though the number of H atoms is the same for all diameters of the H-passivated NWs. Thus, the donor–acceptor system of the H-passivated nanowires is different from that of the OH-passivated nanowires. This may be due to the high electronegativity of the O atoms, which strongly attract electrons, thus reducing the electronic charge that C can attract from Si. Another trend that can be observed is a decrease in the band gap energy as the NW diameter decreases for both H- and OH-passivated NWs, which can be explained by quantum confinement.

The overall results are summarized in Fig. 4, which shows how the electronic band gap evolves as the diameter of the SiCNW is increased. The solid shapes (hexagons for [111], rhombi for [001], and triangles for [112]) represent the H-saturated NWs, while the corresponding empty shapes

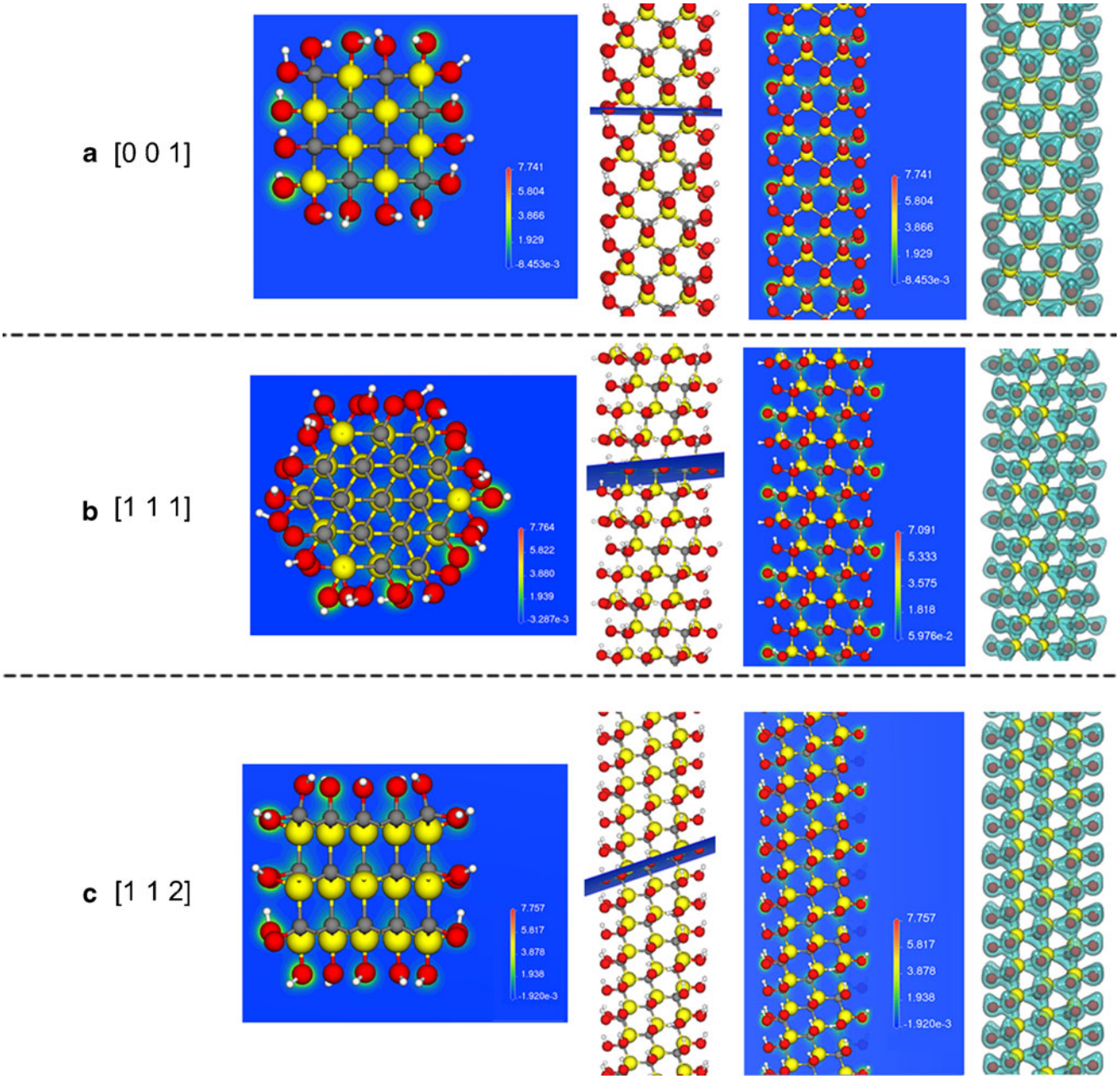

Fig. 5 Electron charge densities of **a** [001]-, **b** [111]-, and **c** [112]-oriented NWs. The *first column* shows a projection of the electron charge density in a plane that passes through only C and O atoms. The side view of this plane is shown in the *second column*. The *third column* presents a {110} plane that passes through C atoms along the nanowire axis. Finally, the isosurface of the electron charge density (isovalue: 0.4 $Å^{-3}$) for the {110} plane examined in **c** is presented in the *fourth column*

represent the OH-terminated ones. It can be seen that both types of NWs show signs of quantum confinement, since the gap decreases as the nanowire diameter increases. However, OH-terminated nanowires show smaller band gaps; in particular, [111] nanowires present different trends for H- and the OH-saturated NWs of diameter 1.065 nm, which can be explained by the increased amount of OH radicals on the surface for the OH-saturated NWs. The NWs that exhibit the widest band gaps are the [001]- and [111]-oriented, H-terminated NWs with diameters of around 0.3 nm. This may be due to the morphology of these nanowires in particular, as in these cases the wire axis can be regarded as a collection of interconnected clusters, creating a confinement effect similar to that present in a 3-D nanostructure; the resulting increased quantum confinement broadens the band gap. This particular morphology is present, but to a lesser degree, for the thicker [001] nanowires, as can be observed in the H-passivated case. However, due to the large number of surface OH bonds compared to the Si–C bonds in the bulk region of the NW, the effects of quasi 3D confinement are reduced for the OH–passivated NWs. The possibility of tailoring the HOMO and LUMO states of SiCNWs by chemically modifying the NW surface and/or adjusting the orientation of the NW could be very useful in band-gap engineering.

Finally, to further explore the reason for this narrowing of the band gap with increased NW diameter, we calculated the electron charge density of each OH-passivated NW. The results are shown in Fig. 5. We first considered a plane that passes through the C and O atoms normal to the wire axis (Fig. 5, first column), and—as expected—the charge density is mainly localized on the O atoms and to lesser degree on the C atoms in all three NW orientations. Then we analyzed a plane along the NW axis that was in the {110} family of planes for each nanowire (see the third column in Fig. 5). In these cases the charge density is concentrated in small planes with different orientations depending on the NW, creating a ropelike structure for the [111] and [112] orientations. To illustrate the charge density across the whole structure, the fourth column in Fig. 5 shows the isosurface with an isovalue of 0.4 $Å^{-3}$ for each NW orientation. These isosurfaces show that in all cases the charge is located around the C atoms and OH radicals, which may be due to the fact that these two species have higher electronegativities than Si, meaning that the Si atoms would transfer most of their charge to these other atoms, creating Si states in the conduction band (as reflected in the DOS shown in Fig. 3).

Conclusions

We have analyzed the effects of changes in nanowire orientation and chemical modifications of the nanowire surface on the electronic properties of SiC nanowires using an ab initio DFT scheme based on the generalized gradient approximation and the supercell technique. The nanowires modeled in this work were grown in the [001], [111], and [112] directions, and either H or OH passivation of the surface dangling bonds was applied. The results show that the nanowires exhibit signs of quantum confinement regardless of the surface passivation technique used, since the electronic band gap decreases as the nanowire diameter increases. The H-passivated nanowires also show significant anistropic effects, as the [001]-oriented nanowire exhibited larger band gaps, probably due to its enhanced quantum confinement, which can be regarded as a quasi 3D confinement. Also, OH passivation was found to have a notable effect on the electronic structures of the NWs, as it narrowed the band gap and introduced flat states near the maximum valence band energy, due to orbitals localized around the O atoms. In addition, the DOS for the OH-passivated nanowires were rather different from those for the H-passivated nanowires; in contrast to the charge transfer seen for the H-passivated nanowires, the charge transfer in the OH-passivated nanowires occurred mostly from Si to O than from Si to C, which may be the reason for the narrower band gaps of the OH-passivated nanowires. These results suggest interesting possibilities for the application of these nanostructures in the field of optoelectronics, as their band gaps can be engineered by adjusting the nanowire orientation and the chemical passivation of the nanowire surface.

Acknowledgments This work was supported by project PICSO12-085 from Instituto de Ciencia y Tecnología del Distrito Federal (ICyTDF), and multidisciplinary project IPN2012-1439 from Instituto Politécnico Nacional. The authors Alejandro Trejo and José Luis Cuevas would like to thank CONACYT for their student scholarships.

References

1. Rostislav AA (2009) Nano-sized silicon carbide: synthesis, structure and properties. Russ Chem Rev 78(9):821–831. doi:10.1070/RC2009v078n09ABEH004060
2. Kim K-S, Chung G-S (2012) Fabrication and characterization of surface type Schottky diode hydrogen sensor using polyaniline/porous 3C-SiC. Synth Met 162(7–8):636–640. doi:10.1016/j.synthmet.2012.02.007
3. Jia YB, Zhuang GL, Wang JG (2012) Electric field induced silicon carbide nanotubes: a promising gas sensor for detecting SO_2. J Phys D Appl Phys 45(6):065305. doi:10.1088/0022-3727/45/6/065305
4. Tian Y, Zheng HW, Liu XY, Li SJ, Zhang YJ, Hu JF, Lv ZC, Liu YF, Gu YZ, Zhang WF (2012) Microstructure and magnetic properties of Mn-doped 3C-SiC nanowires. Mater Lett 76:219–221. doi:10.1016/j.matlet.2012.02.109
5. Liu H, She G, Mu L, Shi W (2012) Porous SiC nanowire arrays as stable photocatalyst for water splitting under UV irradiation. Mater Res Bull 47(3):917–920. doi:10.1016/j.materresbull.2011.12.046
6. Wang HY, Wang YQ, Hu QF, Li XJ (2012) Capacitive humidity sensing properties of SiC nanowires grown on silicon nanoporous

pillar array. Sensors Actuators B Chem 166–167:451–456. doi:10.1016/j.snb.2012.02.087
7. Feng XL, Matheny MH, Zorman CA, Mehregany M, Roukes ML (2010) Low voltage nanoelectromechanical switches based on silicon carbide nanowires. Nano Lett 10(8):2891–2896. doi:10.1021/nl1009734
8. Chiu S-C, Lin W-H, Wu H-C, Youh M-J, Tseng C-L, Chang T-H, Li Y-Y (2012) Silicon carbide nanowire as nanoemitter and greenish-blue nanophosphor for field emission applications. Nanosci Nanotechnol Lett 4(1):72–76. doi:10.1166/nnl.2012.1284
9. Wu R, Zhou K, Wei J, Huang Y, Su F, Chen J, Wang L (2012) Growth of tapered SiC nanowires on flexible carbon fabric: towards field emission applications. J Phys Chem C. doi:10.1021/jp3028935
10. Catellani A, Calzolari A (2012) Functionalization of SiC(110) surfaces via porphyrin adsorption: ab initio results. J Phys Chem C 116(1):886–892. doi:10.1021/jp209072n
11. Choi YY, Kim JG, Park SJ, Choi DJ (2012) Influence of oxygen on the microstructural growth of SiC nanowires. Chem Phys Lett 531:138–142. doi:10.1016/j.cplett.2012.02.009
12. Longkullabutra H, Nhuapeng W, Thamjaree W (2012) Large-scale: synthesis, microstructure, and FT-IR property of SiC nanowires. Curr Appl Phys. doi:10.1016/j.cap.2012.02.032
13. Wu R, Zha B, Wang L, Zhou K, Pan Y (2012) Core-shell SiC/SiO_2 heterostructures in nanowires. Phys Status Solidi A 209(3):553–558. doi:10.1002/pssa.201127459
14. Niu JJ, Wang JN (2009) A novel self-cleaning coating with silicon carbide nanowires. J Phys Chem B 113(9):2909–2912. doi:10.1021/jp808322e
15. Niu JJ, Wang JN (2007) A simple route to synthesize scales of aligned single-crystalline SiC nanowires arrays with very small diameter and optical properties. J Phys Chem B 111(17):4368–4373. doi:10.1021/jp070682d
16. Wu XL, Xiong SJ, Zhu J, Wang J, Shen JC, Chu PK (2009) Identification of surface structures on 3C-SiC nanocrystals with hydrogen and hydroxyl bonding by photoluminescence. Nano Lett 9(12):4053–4060. doi:10.1021/nl902226u
17. Rurali R (2005) Electronic and structural properties of silicon carbide nanowires. Phys Rev B 71(20):205405. doi:10.1103/PhysRevB.71.205405
18. Agrawal BK, Pathak A, Agrawal S (2009) An ab-initio study of metallic and semiconducting [001] SiC nanowires. J Phys Soc Jpn 78(3):034721. doi:10.1143/jpsj.78.034721
19. Wang Z, Zhao M, He T, Zhang H, Zhang X, Xi Z, Yan S, Liu X, Xia Y (2009) Orientation-dependent stability and quantum-confinement effects of silicon carbide nanowires. J Phys Chem C 113(29):12731–12735. doi:10.1021/jp903736v
20. Mirzaei M, Mirzaei M (2010) A computational study of atomic oxygen-doped silicon carbide nanotubes. J Mol Model 17(3):527–531. doi:10.1007/s00894-010-0751-3
21. Saha S, Sarkar P (2012) Tuning the HOMO–LUMO gap of SiC quantum dots by surface functionalization. Chem Phys Lett 536:118–122. doi:10.1016/j.cplett.2012.03.107
22. Vörös M, Deák P, Frauenheim T, Gali A (2010) The absorption of oxygenated silicon carbide nanoparticles. J Chem Phys 133 (6):064705. doi:10.1063/1.3464482
23. Dionízio Moreira M, Venezuela P, Schmidt TM (2008) The effects of oxygen on the surface passivation of InP nanowires. Nanotechnology 19(6):065203. doi:10.1088/0957-4484/19/6/065203
24. Cuevas JL, Trejo A, Calvino M, Carvajal E, Cruz-Irisson M (2012) Ab-initio modeling of oxygen on the surface passivation of 3CSiC nanostructures. Appl Surf Sci. doi:10.1016/j.apsusc.2012.03.175
25. Hammer B, Hansen LB, Nørskov JK (1999) Improved adsorption energetics within density-functional theory using revised Perdew–Burke-–Ernzerhof functionals. Phys Rev B 59 (11):7413–7421
26. Vanderbilt D (1990) Soft self-consistent pseudopotentials in a generalized eigenvalue formalism. Phys Rev B 41(11):7892–7895. doi:10.1103/PhysRevB.41.7892
27. Clark SJ, Segall MD, Pickard CJ, Hasnip PJ, Probert MIJ, Refson K, Payne MC (2005) First principles methods using CASTEP. Z Kristallogr 220:567–570. doi:10.1524/zkri.220.5.567.65075
28. Monkhorst HJ, Pack JD (1976) Special points for Brillouin-zone integrations. Phys Rev B 13(12):5188–5192. doi:10.1103/PhysRevB.13.5188
29. Pfrommer BG, Côté M, Louie SG, Cohen ML (1997) Relaxation of crystals with the quasi-Newton method. J Comput Phys 131 (1):233–240. doi:10.1006/jcph.1996.5612
30. Sk MA, Ng M-F, Yang S-W, Lim KH (2011) Water induced electrical hysteresis in germanium nanowires: a theoretical study. Phys Chem Chem Phys 13(24):11663. doi:10.1039/c1cp20228f